

CURVELET ANALYSIS OF KYMOGRAPH FOR TRACKING BI-DIRECTIONAL PARTICLES IN FLUORESCENCE MICROSCOPY IMAGES

Nicolas Chenouard¹, Johanna Buisson², Isabelle Bloch³, Philippe Bastin², Jean-Christophe Olivo-Marin¹

¹Institut Pasteur, Unité d'Analyse d'Images Quantitative; CNRS URA 2582, Paris, France

²Institut Pasteur, Unité de Biologie Cellulaire des Trypanosomes; CNRS URA 2581, Paris, France

³TELECOM ParisTech, CNRS UMR 5141 LTCI, Paris, France

ABSTRACT

In this paper we present a new procedure for tracking bi-directional objects in kymographs. The proposed technique is based on a novel adaptive and directional band-pass filtering method which allows us to separate particles which move in opposite directions. The filtering method exploits the curvelet analysis of the kymograph image to automatically adapt to the objects trails characteristics and select oriented features. The separation of bi-directional objects in separated images allows us to reliably detect and track fluorescent particles in fluorescence image sequences, despite numerous crossroad points in the kymograph space. The new abilities provided by the proposed technique are highlighted by the analysis of biological images which were previously impossible to analyze reliably.

Index Terms— Curvelet transform, Kymograph, Particle tracking, Multiple Hypothesis Tracking (MHT)

1. INTRODUCTION

Tracking nanometric scale particles over time is the method of choice to characterize sub-cellular mechanisms since it provides robust and accurate information on sub-cellular dynamics [1]. Over the past years a number of automatic approaches have been proposed to recover the successive positions of particles in microscopy image sequences (see [2, 3] and references therein). A number of particle tracking methods rely on a two-steps procedure: (1) detect the spot positions in each frame, (2) link the sets of positions between subsequent frames according to the detected particles. The latter step is generally referred as the *association problem* between the detected positions and the set of tracks.

In a number of biological applications, such as particle tracking along microtubules and axons, numerous objects go through common paths. In this case, exploiting the redundancy of the trajectories is a possible manner to reduce the complexity of the tracking problem by imposing tracks to go through fixed spatial paths. The kymograph analysis exploits this idea in an efficient manner: the spatio-temporal volume is projected to a 2D space called kymograph (or kymogram), where one axis represents the position along the reference path, and the second direction is the time point in the image sequence. When particles move slowly along the reference path, they yield a continuous fluorescent trail in the kymograph space which can be analyzed to recover particle trajectories. For instance, in [4] one kymograph is built for each single fluorescent

object, for which the trajectory is extracted by a Bayesian estimation technique. In [5] the extraction of multiple trajectories from a single kymograph is achieved by using an automatic line extraction algorithm. However, crossing trails cannot be resolved with the latter method and it is proposed to split tracks into small segments to avoid false links when conflicts are detected. Hence, there exists yet no tracking method handling robustly multiple particles which are frequently crossing in the kymograph image.

In this paper we propose a method to track reliably multiple particles despite numerous cross-points in the kymograph space. The method relies on a novel band-pass filtering technique which is both directional and adaptive to the kymograph features. We propose here to exploit the curvelet domain representation [7] of the kymograph to separately extract the frequency components corresponding to the trails of particles showing anterograde and retrograde motion. While some methods have been proposed for directional components separation based on the estimation of local orientations (e.g. [6]), our technique automatically achieves the separation by selecting the frequency wedges which fit the anterograde and retrograde particle trails, respectively. As a result, trails with opposite directions are reconstructed in different images in which the signal-to-noise ratio (SNR) is improved. The independent extraction of anterograde and retrograde trails and the improved SNR allow us to track particles in the separated images in a robust manner. This point is illustrated with the tracking of numerous crossing cargos in the trypanosome flagellum using a robust Bayesian tracking technique [8].

The outline of the paper is as follows: in Section 2 we describe the kymograph analysis based on the curvelet transform for separating bi-directional particles. We then provide in Section 3 experimental results of cargo tracking in microscopy images of the trypanosome. Finally, we summarize and discuss our proposals.

2. KYMOGRAPH ANALYSIS WITH THE CURVELET TRANSFORM

2.1. Kymograph representation of an image sequence

The kymograph \mathcal{K} is a 2D representation of the intensity fluctuations over time along a reference line \mathcal{L} in 2D (or 3D) space. Each line of \mathcal{K} corresponds to the observed intensities along \mathcal{L} at a given time point. At each time point k the intensity value in the k th image is sampled along \mathcal{L} with a fixed step δ . For instance, we show in Figure 1 a kymograph extracted from a microscopy image sequence of a trypanosome parasite. The kymograph values $\mathcal{K}(t, d)$ give the intensity value at time t at position $d \times \delta$ on the trypanosome flagellum (\mathcal{L}), a long tubular structure. In \mathcal{K} , hundreds of fluorescent trails with various properties can be observed: some are very regular and

N.Chenouard is funded by C'Nano IdF.

Corresponding authors: N. Chenouard and J.C. Olivo-Marin

Correspondence: nicolas.chenouard@gmail.com, jcolivo@pasteur.fr

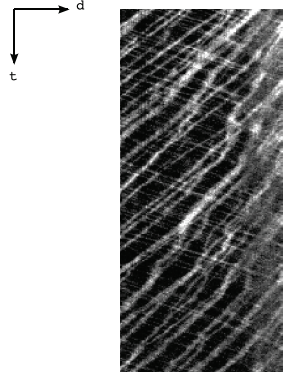


Fig. 1. Kymograph image extracted from a microscopy image sequence of the trypanosome. Fluorescent trails correspond to particle trajectories along the flagellum.

thin lines, other are thick with irregular curvature. The trails in \mathcal{K} correspond to fluorescent particle trajectories along \mathcal{L} : a regular line indicates a particle moving with a constant velocity which is proportional to the line's slope, and a more complex pattern corresponds to a particle with varying motion types.

In Figure 1 we show that many trails do cross in the kymograph space, hence reflecting the bi-directionality of the particles along \mathcal{L} . The numerous crossroads in \mathcal{L} prevent the use of procedures based on line extraction techniques such as [5]. On the other hand, for two-step tracking approaches, the association problem is ill posed since standard detection methods produce a single detection for several crossing particles at crossroad points.

2.2. Separation of anterograde and retrograde movements in the curvelet domain

In order to solve the issue of bi-directional particles in the kymograph space, we present next a new method to split anterograde and retrograde trajectories into two independent kymograph images. The separated kymographs can then be processed separately with a standard tracking procedure.

2.2.1. Directional image analysis with the curvelet transform

The 2D curvelet transform allows the directional and multiscale analysis of an image by decomposing it as a combination of segments of various length and width [9]. The digital curvelet decomposition is linear and takes as input Cartesian arrays of the form: $f[t_1, t_2]$, $0 \leq t_1 < n_1$, $0 \leq t_2 < n_2$. The output is a set of coefficients $c(j, l, k)$ at each scale j and angle l which can thus be expressed as:

$$c(j, l, k) = \sum_{0 \leq t_1 < n_1, 0 \leq t_2 < n_2} f[t_1, t_2] \phi_{j,l,k}[t_1, t_2] \quad (1)$$

where each $\phi_{j,l,k}$ is a digital curvelet waveform. Equation 1 can be rewritten in matrix form as:

$$X = Y\Phi, \text{ and } X = \bar{\Phi}^*Y, \quad (2)$$

where X is the column vector of the curvelet coefficients and Y is the image concatenated in a column vector. The matrix Φ contains the curvelet waveforms and is called the analysis operator, while $\bar{\Phi}^*$

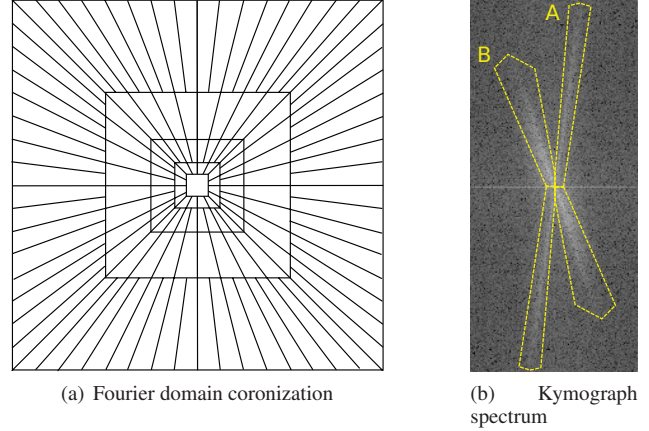


Fig. 2. Fourier domain analysis. On the left-hand side we show the domain coronization that is achieved by the curvelet decomposition when omitting the wedge overlaps. On the right-hand side, we show the frequency spectrum of the kymograph shown in Figure 1. We indicate in yellow that most meaningful information of the kymograph is included in two sectors corresponding to few curvelet wedges.

corresponds to the synthesis operator. In practice, neither the digital waveforms nor the matrices Φ and $\bar{\Phi}^*$ are built: they are implicitly defined by the algorithm. The wrapping implementation of the curvelet transform [7] relies on the computation of the coefficient $c(j, l, k)$ in the Fourier domain as:

$$c(j, l, k) = \int \hat{f}(\omega) \tilde{U}_j(S_{\Theta_l}^{-1}\omega) e^{i\langle b, \omega \rangle} d\omega, \quad (3)$$

where $\tilde{U}_j(S_{\Theta_l}^{-1}\omega)$ is a smooth frequency window which is supported on a parallelepipedal region (the matrix S_{Θ_l} is a shear matrix of angle Θ_l , and $b \simeq (k_1 2^{-j}, k_2 2^{-j/2})$ with $k = (k_1, k_2)$). In practice, the frequency domain is tiled with a set of oriented smooth windows $\tilde{U}_{j,l}$, called *wedges*. The wedge decomposition consists in a coronization of the frequency domain based on concentric squares and shears which are slightly overlapping. We illustrate the coronization in Figure 2(a) by omitting the overlaps between wedges.

2.2.2. Kymograph Fourier analysis

We show in Figure 2(b) the frequency spectrum of the kymograph built previously in Fig. 1. Interestingly, the spectrum shows well identified sectors, grossly delineated in yellow in Figure 2(b), which contain most of the meaningful information. Each of these two sectors corresponds to a different class of fluorescent trails in \mathcal{K} :

- Sector A is close to the vertical axis, it thus corresponds to trails with a slope value close to 0 in \mathcal{K} (high velocity). The regularity of the trails, and the nearly constant velocity of the particle motion, yield a thin sector in the Fourier domain. This sector corresponds to retrograde trails in \mathcal{K} .
- Sector B is much wider than the sector A, which indicates that the corresponding movements are less regular. It corresponds to particles showing anterograde motion.

The two frequency sectors, A and B, are both contained in different wedges. We thus propose to take advantage of the frequency tiling achieved by the curvelet decomposition to isolate the two frequency

components, thereby separating bi-directional trails. The sectors are also embedded in only few wedges, we thus automatically fit the wedge selection to the sectors to exclude noise-only components and improve the SNR of the reconstructed images.

2.2.3. Adaptive band-pass filtering by wedge selection

We first apply the curvelet decomposition to the kymograph image \mathcal{K} to obtain the representation X such that $\mathcal{K} = \bar{\Phi}^* X$. Our goal is to design two matrix operators M_a and M_r , which select the curvelet coefficients corresponding to anterograde and retrograde trails in \mathcal{K} , respectively. The separated images \mathcal{K}_a and \mathcal{K}_r are then obtained by applying the backward curvelet transform to the masked coefficients as follows:

$$\mathcal{K}_a = \bar{\Phi}^* M_a X, \quad \mathcal{K}_r = \bar{\Phi}^* M_r X. \quad (4)$$

The proposed approach is to select wedges which correspond to the desired trail directions and obtain a directional band-pass filtering of \mathcal{K} .

Quadrant selection. As shown in Fig. 2(b) the two frequency sectors of interest lie in different quadrants of the Fourier domain. Hence, wedges can be selected according to the quadrant in which they are contained. We note Q_a and Q_r the binary matrices selecting curvelet coefficients in the frequency quadrant corresponding to anterograde and retrograde motion, respectively. The lowest frequency wedge is also discarded by Q_a and Q_r . Applying the operators Q_a and Q_r to X allows us to separate anterograde and retrograde moving particles in two independent images, and to flatten the kymograph background.

Adaptive wedge selection. The quality of the reconstructed kymograph images \mathcal{K}_a and \mathcal{K}_r can be improved by discarding wedges that do not contain meaningful information for particle tracking. Indeed, the pixel wise noise corrupting \mathcal{K} is uniformly distributed in the Fourier domain, while the particle signal is restricted to the sectors A and B . We thus propose to adaptively detect the set of wedges representing particle trails. To do so, we compute the normalized mean energy for each wedge at each scale:

$$e_{j,l}^2 = \frac{1}{n_{j,l}} \sum_k \frac{c(j,l,k)^2}{\sigma_{j,l}^2}, \quad (5)$$

where $n_{j,l}$ is the number of wavelet coefficients $c(j,l,k)$ corresponding to the wedge $\tilde{U}_{j,l}$, with l the index of the wedge at scale j . The normalizing term $\sigma_{j,l}^2$ is the energy scaling factor for the wedge $\tilde{U}_{j,l}$ ($\sigma_{j,l}^2$ is estimated by computing the energy of the wedge $\tilde{U}_{j,l}$ when the curvelet transform is applied to an image of unit energy). After normalization, the range of the energy values can be compared between wedges with different orientations and from different scales. We propose to cluster the histogram of the wedge energy for each scale in two classes: wedges with high energy that correspond to a meaningful information, and low energy wedges which correspond to artifacts and noise only. The histogram segmentation method in [10] provides an energy threshold t_j for each scale j which is used to design a binary matrix W for the selection of the curvelet coefficients. A coefficient in the wedge $\tilde{U}_{j,l}$ is selected if $e_{j,l}^2 > t_j^2$; it is discarded otherwise.

Finally, the image separation matrices M_a and M_r are obtained by combining the quadrant separation rule and the adaptive band-pass filtering procedure in the following way:

$$M_a = Q_a W, \quad M_r = Q_r W. \quad (6)$$

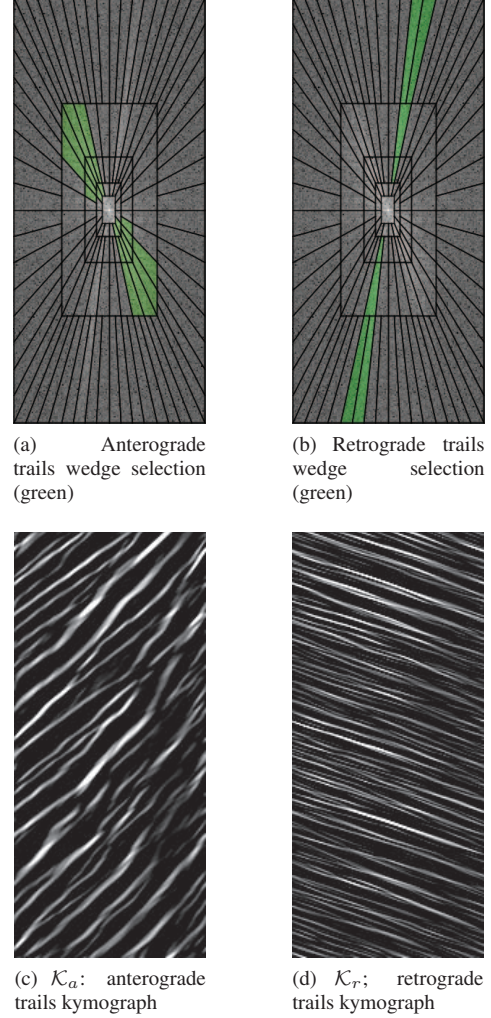


Fig. 3. Separation of bi-directional trails with adaptive band-pass filtering.

In Figures 3(a) and 3(b) we show the band-pass filtering illustrating the selection of the curvelet coefficients when the proposed matrices, M_a and M_r , are used. We show that the selected wedges are automatically fitted to the spectrum of the kymograph, hence achieving an efficient band-pass filtering. In Figures 3(c) and 3(d) we give the kymographs \mathcal{K}_a and \mathcal{K}_r obtained by applying Equation 4 with the proposed M_a and M_r matrices. The anterograde and retrograde fluorescent trails are well separated in \mathcal{K}_a and \mathcal{K}_r , hence proving the efficiency of the quadrant selection procedure. As compared to the original kymograph \mathcal{K} (Fig. 1), the signal quality is improved in \mathcal{K}_a and \mathcal{K}_r , which illustrates the ability of the wedge selection procedure to adapt to the signal spectrum and discard artifacts.

An alternative approach to adaptive band-pass filtering would be to denoise curvelet coefficients and to discard the coefficients induced by the noise. The benefits of the proposed method over the denoising approach is however to keep low amplitude coefficients originating from low intensity particles.

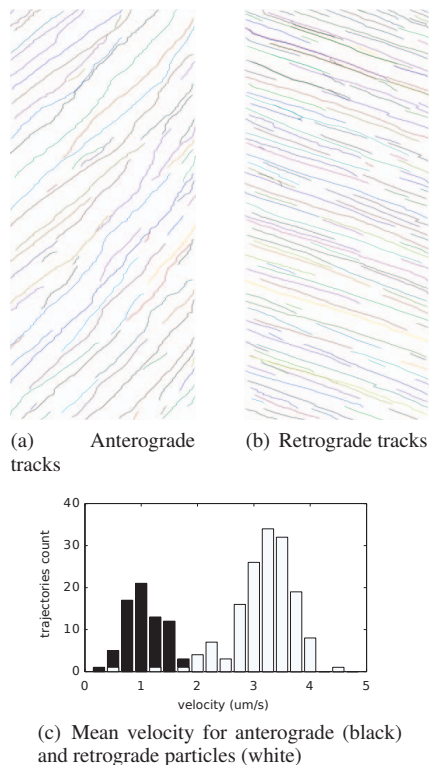


Fig. 4. Tracks built by the proposed procedure. Crossroad points in the original kymograph do not corrupt the track construction, which allows one to measure accurately particle velocity.

3. CARGO TRACKING IN THE TRYPANOSOME FLAGELLUM

We have applied the bi-directional tracking technique to the kymograph image of protein cargos moving along trypanosome flagella (Fig 1). The separated kymographs, \mathcal{K}_a and \mathcal{K}_r , have then been processed independently to identify the cargos tracks. The tracking problem is facilitated in the separated kymographs since the particle signal is enhanced and no intersection occurs between bi-directional trails. For each kymograph, we have adopted a two-step procedure: (1) we identify putative particle positions by detecting a set of relevant local intensity maxima [10] which are analysed to achieve a sub-pixel accuracy, (2) the set of positions are linked through time thanks to a statistical tracking algorithm [8] which automatically discards wrong detections and compensates for missing detections thanks to particle motion modeling. As shown in Figures 3(c) and 3(d), the separated kymographs provide as well a clear representation of the particle trajectories. Trajectories visualization and correction by the user is thus highly facilitated and accelerated if needed. A total of 60 kymographs, coming from 8 separate experiments, has already been successfully analysed, demonstrating that the system is robust and can be used for extensive biological analyses.

We show in Figure 4(a) and 4(b) the cargo trajectories obtained by the proposed automatic tracking technique after the computer-aided interactions with an operator. While no existing solution was able until now to analyze reliably trypanosoma kymographs such as Fig. 1, our proposed solution provides the accurate trajectories of 240

particles (89 anterograde and 151 retrograde cargos) in just a few minutes. This information can be extensively analyzed to understand biological phenomena, as illustrated by the velocity histogram, shown in Figure 4(c), which we have computed from the proposed method results. The computed histogram proves that anterograde particles are much faster than retrograde ones.

4. SUMMARY

In this paper we have presented a novel solution to the issue of tracking bi-directional particles along a spatial line. We have proposed to apply a new adaptive and directional band-pass filtering method to kymograph images in order to separate particles which move in opposite directions. The proposed technique relies on the automatic selection of relevant curvelet wedges based on the automatic analysis of their energy. The benefits of the proposed method have been illustrated with the tracking of protein cargos along the trypanosome flagellum. The adaptive-filtering technique allows us to accurately identify particle trajectories despite the high number of crossroad points in the kymograph image, hence bringing a new robust tool to study such biological data.

5. REFERENCES

- [1] B. Brandenburg and X. Zhuang, "Virus trafficking - learning from single-virus tracking," *Nature Reviews Microbiology*, vol. 5, no. 3, pp. 197–208, 2007.
- [2] E. Meijering, I. Smal, and G. Danuser, "Tracking in molecular bioimaging," *IEEE Signal Processing Magazine*, vol. 23, no. 3, pp. 46–53, 2006.
- [3] N. Chenouard, A. Dufour, and J.-C. Olivo-Marin, "Tracking algorithms chase down pathogens," *Biotechnology Journal*, vol. 4, no. 6, pp. 838–845, 2009.
- [4] I. Smal, I. Grigoriev, A. Akhmanova, W. J. Niessen, and E. Meijering, "Accurate estimation of microtubule dynamics using kymographs and variable-rate particle filters," in *Annual Intern. Conf. IEEE Eng. in Medicine and Biology Soc. - EMBC*, 2009.
- [5] V. Racine, M. Sachse, J. Salermo, V. Fraisier, A. Trubil, and J.-B. Sibarita, "Visualization and quantification of vesicle trafficking on a three-dimensional cytoskeleton network in living cells," *Journal of Microscopy*, vol. 225, no. 3, pp. 214–228, 2006.
- [6] Til Aach and Ingo Stuke, "Estimation of multiple local orientations in image signals," in *In Proc. IEEE Int. Conf. Acoustics Speech and Signal Processing*, 2004, pp. 553–556.
- [7] E. J. Candes, L. Demanet, D. L. Donoho, and L. Ying, "Fast discrete curvelet transforms," *SIAM Journal on Multiscale Modeling and Simulation*, vol. 3, pp. 861 – 899, 2006.
- [8] N. Chenouard, I. Bloch, and J.-C. Olivo-Marin, "Multiple hypothesis tracking in cluttered condition," in *16th IEEE Intern. Conf. Image Processing - ICIP*, 2009.
- [9] J.-L. Starck, E. J. Candes, and D. L. Donoho, "The curvelet transform for image denoising," *IEEE Trans. Image Processing*, vol. 11, no. 6, pp. 670–684, 2002.
- [10] N. Otsu, "A Threshold Selection Method from Gray-level Histograms," *IEEE Trans. Systems Man and Cybernetics*, vol. 9, no. 1, pp. 62–66, 1979.